END-PLATE POTENTIALS IN A MODEL MUSCLE FIBER

Corrections for the Effects of Membrane Potential on Currents and on Channel Lifetimes

W. VAN DER KLOOT AND I. S. COHEN
Department of Physiology and Biophysics, Health Sciences Center, State University of New York at Stony Brook, Stony Brook, New York 11794

ABSTRACT At the neuromuscular junction, the end-plate potential is generated by a conductance increase in the end-plate membrane. The end-plate depolarization brings the membrane potential toward the reversal potential, which diminishes the driving force for inward current flow. A. R. Martin (1955, *J. Physiol.* [*Lond.*]. 130:114–122) devised a simple formula to correct end-plate potential amplitudes for a diminished driving force based on a purely resistive model of the end-plate membrane. The model ignores the membrane capacity, the complexity of the equivalent circuit for a muscle fiber, the variation in channel lifetimes with changes in membrane potential, and the extension of the end plate along a length of the cable. We have developed a model that incorporates all of these features. The calculations show that Martin's correction is, in theory, quite satisfactory for a cable that has the characteristics of a muscle fiber unless the recording is made at a distance from the site of inward current flow. However, there is a discrepancy between models of the frog neuromuscular junction and the available experimental data, which suggests that the end-plate depolarization produced by a given current is greater than expected from their model.

INTRODUCTION

At the neuromuscular junction acetylcholine (ACh) opens channels in the end-plate membrane through which a depolarizing current normally flows. The equilibrium potential for the endplate current, E_{eq}, taken as the difference between the reversal potential of −5 mV (Lewis, 1979) and a resting membrane potential of −80 mV is 75 mV. The inward current generates an end-plate potential, E_{epp}, which we define as the difference between the potential at the activated end plate and the resting potential, so a depolarization is seen as a positive change in potential. As the E_{epp} rises, it approaches E_{eq} so the driving force for the inward current decreases. Consequently, the relation between the maximum end-plate conductance, g_j, caused by the ACh and the end-plate potential, E_{epp}, is nonlinear.

Martin (1955) proposed a correction for this nonlinear behavior, based on a simple equivalent circuit containing only resistances. The corrected end-plate potential, E'_{epp} is given by

$$E'_{epp} = E_{epp}/(1 - E_{epp}/E_{eq}). \quad (1)$$

This correction has been used frequently for calculating the number of quanta released following nerve stimulation, which is then given by E'_{epp} divided by the amplitude of the mean miniature end-plate potential (epp). However, the correction is a simplification because it ignores membrane capacity. Several attempts have been made to improve the correction in this regard (Adams, 1976; Bennett et al., 1976; Martin, 1966; Stevens, 1976; Williams and Bowen, 1974). But it is difficult to evaluate whether these elaborations are necessary or effective. Clearly the equivalent circuit for a muscle fiber is more complicated then that of a simple cable, owing to the T-tubule system (Falk and Fatt, 1964; Gage and Eisenberg, 1969). It has been found that the lifetime of the ACh-gated channel depends on E_m, with depolarization the mean channel lifetime decreases (Magleby and Stevens, 1972; Anderson and Stevens, 1973; Neher and Sakmann, 1976). A further consideration is that the mammalian end plate is relatively compact, but the frog's end plate extends along the cable (Kuno et al., 1971). Consequently, we decided to model an end plate on a muscle fiber, taking each of these complications into account.

McLachlan and Martin (1981) published the results of experiments in which on the same fiber the end-plate potential amplitude was compared with the peak end-plate current. They compared their results to an analytical solution of the response of a muscle cable model with rectangular current pulses lasting 1.5 ms and concluded that the measured end-plate potential amplitudes were greater then those predicted. Ginsborg et al. (1982) further developed this model, by a series of approximations, so they could calculate the response to any arbitrary time course of current flow. Our results agree with theirs for similar conditions; however, our method allows us to calculate the

voltage change at any point along the cable-to-current inflow, and current can enter at any number of different points along the cable.

MODEL OF THE END PLATE ON A MUSCLE CABLE

Muscle Cable

Our model is based on the equivalent circuit for a muscle fiber developed by Adrian and Almers (1973), which is diagrammed in Fig. 1. The behavior of this cable is described by

$$(1/r_a) \cdot [d^2E_m(t)/dx^2] = E_m(t)/r_m + dE_m(t)/dt \cdot c_m + dE_T(t) \cdot c_T + [E_{eq} - E_m(t)]/r_j(t), \quad (2)$$

where the symbols are defined in Fig. 1 and its caption and

$$dE_T/dt = [E_m(t) - E_T]/r_S. \quad (3)$$

The values used in the calculations are also given in the caption to Fig. 1.

Time Course of the End-Plate Conductance Change

The time course of the resistance change triggered by ACh at the end-plate, r_j, was calculated by the equations developed by Magleby and Stevens (1972). The conductance of the junctional channels, $g_j(t) = 1/r_j$ is given by

$$dg_j(t)/dt = B[E_m(t)] \cdot W(t) - A[E_m(t)] \cdot g_j(t), \quad (4)$$

where

$$A(E_m) = 1.57 \cdot \exp(0.00682 \cdot E_m), \quad (5)$$

and

$$B(E_m) = 0.35 \cdot \exp(0.00315 \cdot E_m). \quad (6)$$

The driving function $W(t)$ reflects the number, in arbitrary units, of the receptors complexed with ACh and in the closed configuration. We use the following approximation for the curve showing the behavior of $W(t)$ given by Magleby and Stevens (1972)

$$W(t) = 21{,}000 \cdot t, \qquad t \le 0.00018 \quad (7)$$

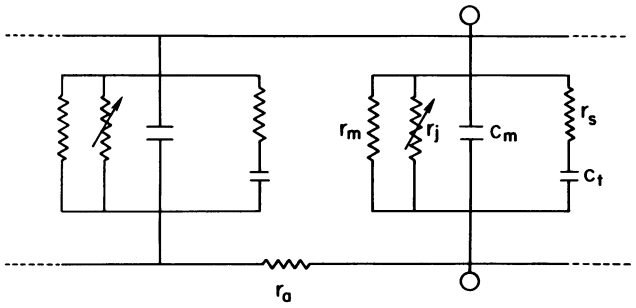

FIGURE 1 The model cable used in the calculations. The values used for the calculations were R_m = 1,500 ohm cm^2, R_s = 600 ohm cm^2, R_a = 170 ohm cm, $c_m = 1 \times 10^{-6}$ F/cm^2, and $C_t = 6 \times 10^{-6}$ F/cm^2. The fiber radius, a, was taken as 30×10^{-4} cm. Then $r_m = R_m/2 \cdot \pi \cdot a$; $r_a = R_a/\pi \cdot a^2$; $r_s = R_s/2 \cdot \pi \cdot a$; $c_m = C_m \cdot 2 \cdot \pi \cdot a$; $c_t = C_T \cdot 2 \cdot \pi \cdot a$. Values for r_j were calculated as described in the text.

and

$$W(t) = 3.8 \cdot \exp[-(t - 0.00018)/0.00027)], \quad t \ge 0.00018 \quad (8)$$

where t is the time in seconds.

Methods for Solving the Equations

Eq. 2 was rewritten as difference equations according to the Crank-Nicholson method for 100 points along the cable (McCracken and Dorn, 1964; Moore et al., 1975), the points were separated by 0.01 cm. The junction was taken to be at point 50. The resulting set of simultaneous equations form a tridiagonal matrix that was solved by Gaussian elimination (Carnahan et al., 1969). Eqs. 3 and 4 were solved by a fourth-order Runga-Kutta method. The computations were done on a PDP 11/03 or 11/23 computer (Digital Equipment Corp., Marlboro, MA).

Time Course of End-Plate Channel Opening

From the previous computations we obtain the relation between the end-plate current and the the epp amplitude. However, the relation that is most pertinent is that between the quantity of ACh acting on the end plate and the end-plate current (epc). The ACh opens channels in the membrane; the conductance depends on how many channels are open at any given moment. Therefore we want to calculate the relation between the total number of channels that have opened and the epp. Cohen et al. (1981) showed that the number of channels opened per unit time, $n(t)$ is given by

$$n(t) = (dI/dt + I/\tau_c)/i_1, \quad (9)$$

where I is the end-plate current, τ_c is the mean channel lifetime, and i_1 is the current through an open channel. The time course of an end-plate current at a fixed E_m was calculated by Eqs. 4–8. The pattern of channel opening was then calculated by Eq. 8. The fraction of channels closing in a small time interval, Δt, is given by

$$F_o = (\Delta t/\tau_c). \quad (10)$$

Therefore, the number of open channels at any given time can be computed and used to determine the end-plate conductance, the end-plate current, and finally the epp.

RESULTS

End-Plate Currents and Calculated End-Plate Potentials

Fig. 2 is an example of a calculated change in the end-plate conductance and the resulting change in E_m at several points along the muscle cable. The results are similar to actual data (Fatt and Katz, 1951, their Fig. 5). Fig. 3 shows the relationship between the maximum, g_j, and the peak of the calculated end-plate potential, E_{epp}. Also shown is the correction by Martin's method (Eq. 1), which clearly shows a direct proportion between the maximum conductance and the epp amplitude.

Effects of Lengthened End-Plate Currents

We thought that the correction might not be as effective when the end-plate current was prolonged, as occurs at low temperature. Therefore, we repeated the calculations with

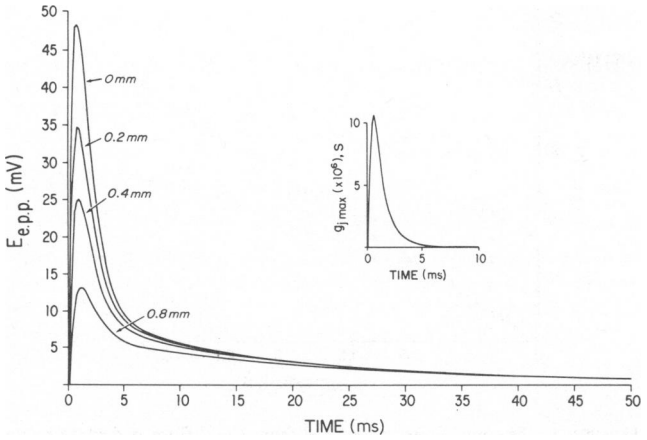

FIGURE 2 The insert shows the time course of a conductance change at point 0 on the model cable. Also shown are the calculated changes in E_m, resulting from the conductance change, at four different points along the cable.

the value of $A(E_m)$, from Eq. 4, decreased by a factor of three, as might occur with a 10°C drop in the temperature. The correction was still effective. However, Fig. 4 shows the calculated peak, E_{epp}, at low temperature at a point on the membrane 0.3 mm from the site of inward current flow plotted as a function of the peak, g_j. Also shown are the values of the E_{epp} corrected by Martin's method. Obviously the correction is much less effective at a distance from the end plate, because there the membrane capacity plays a larger role in determining the magnitude of the response.

We also repeated the calculations with the parameters for room temperature, taking into account the changes in R_m expected from the muscle membrane as a result of the voltage dependence of the K^+ channel (Adrian and Peachey, 1973). The results were not notably different from those already shown.

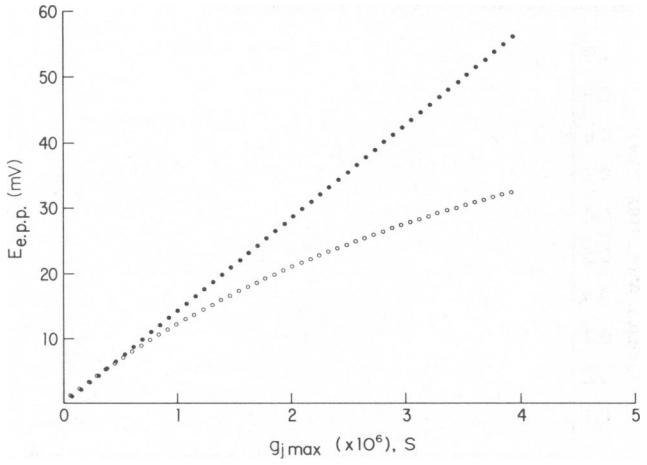

FIGURE 3 The peak amplitude of the calculated epp at point zero on the cable, plotted as a function of the maximum conductance change. The open circles (○) show the direct results of the calculation. The filled circles (●) show the amplitudes as corrected by Martin's method (Eq. 1). The correction establishes a linear relation between the peak of the conductance change and the peak epp.

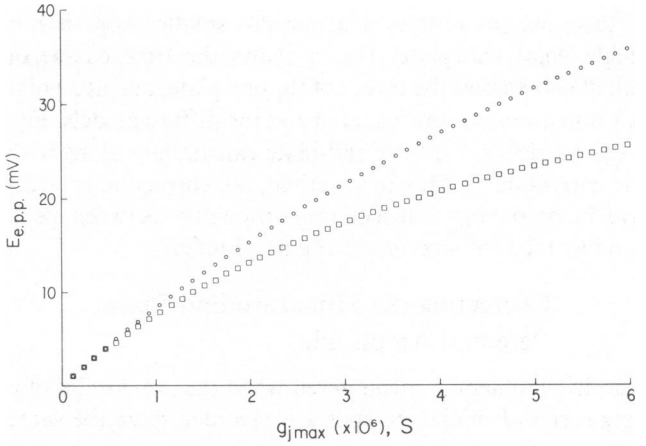

FIGURE 4 The calculated peak amplitudes of the epp at a point 0.03-cm down the cable from the point of current inflow as a function of the maximum conductance change at point 0 (□). The data corrected by Martin's method are shown by the circles. Notice that the correction does not establish a linear relation between the maximum conductance and amplitude, when the amplitude is measured away from the point of current inflow.

Effects of a Diffuse End Plate

The frog end plate is diffuse, it extends for up to 0.5 of a λ along the muscle fiber. Therefore, to test the importance of the diffuse nature of the end plate, the calculations were repeated with current inflow at seven points along the model cable. Fig. 5 shows the results of these calculations along with results from calculations of the type presented earlier, in which current inflow is at a single point. The results show that for a given total conductance change, a

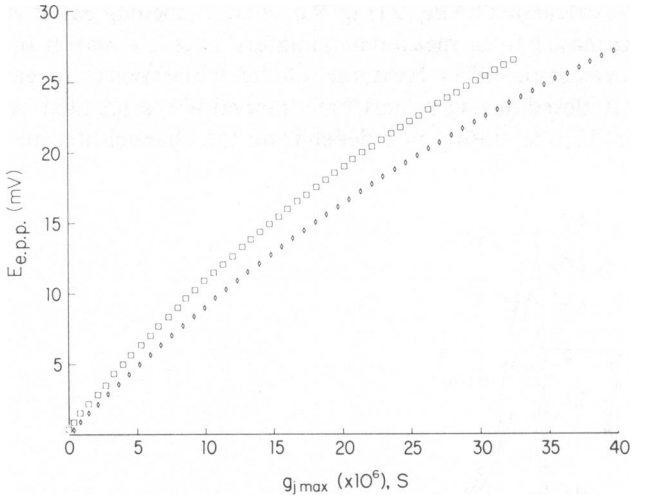

FIGURE 5 The calculated peak amplitudes of epps as a function of the maximum conductance change for a single point (□) and for a diffuse (◇) model. For the single point model the conductance change was at one location (point 50). For the diffuse model the conductance change was at seven points along the cable (47–53), the peak epp was that calculated for point 50. In the diffuse model the maximum conductance change was the sum of the individual maxima at each of the seven points of inward current flow.

diffuse end plate gives a somewhat smaller epp than a single point end plate. Fig. 6 shows the time course of calculated epps at the center of the end plate, and at a point 0.3-mm away, for the centered and the diffuse models. Fig. 7 summarizes the diffuse end-plate calculations along with the correction by Martin's method; the correction is effective in producing a direct proportionality between peak conductance and maximum epp amplitude.

Correcting the Miniature End-Plate Potential Amplitudes

Another problem is encountered when the amplitudes of a long series of miniature epps are recorded from the same junction, if the membrane potential depolarizes during the recording period. Katz and Thesleff (1957) recorded miniature epp peak amplitudes, $E_{\text{miniature epp}}$, and resting membrane potential, E_m. All of the amplitudes are then corrected to a standard membrane potential, E_s, by multiplying by $(E_s - E_{eq})/(E_m - E_{eq})$. Fig. 8 shows calculated maximum amplitudes of miniature epps at different values of E_m. Fig. 8 also shows the corrected miniature epp amplitudes for a $E_m = -80$ mV; the method of correction works quite well, over a 70-mV range the corrected values are always within 12% of the target.

Channel Lifetimes and End-Plate Potentials

The variable that remained to be explored was the effect of membrane potential on channel lifetime (see Introduction). This was done by first calculating the time course of an end-plate current at constant E_m by Eq. 4. Then the pattern of the channel opening responsible for the current was calculated by Eq. 9 (Fig. 9 *a*; channel opening patterns calculated from measured miniature epcs are shown by Cohen et al., 1981). Next, the fraction of the open channels that closed during a short time interval was calculated by Eq. 10; the closing rate depends on the channel lifetime,

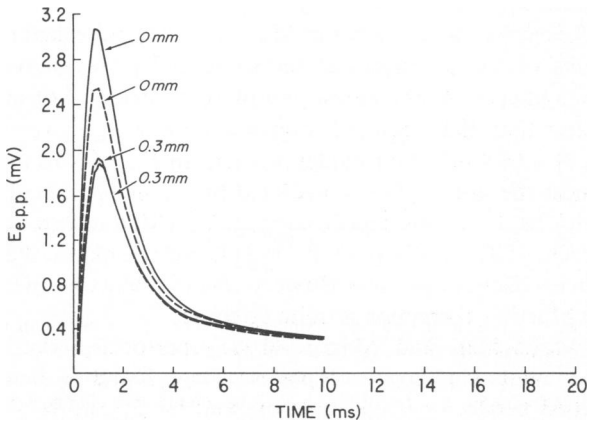

FIGURE 6 Examples of the time course of calculated single point and diffuse epps. The approach is described in the legend to Fig. 5. —, single point current inflow; · · ·, diffuse model.

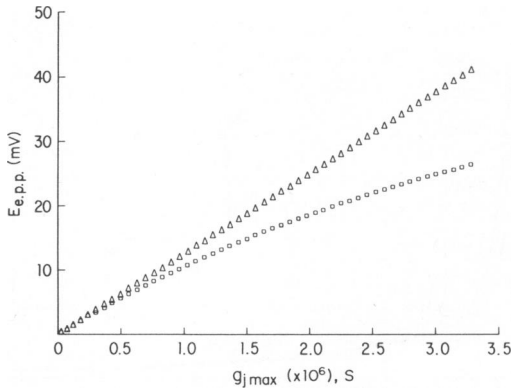

FIGURE 7 The peak epps calculated from the diffuse end-plate model (□), along with the correction by Martin's method (◇). The correction is excellent.

which is a function of the membrane potential. Summing channel opening and closing gives the number of open channels, and therefore the end-plate conductance, at any given moment.

Fig. 9 *b*, *c* show the calculated epc and the epp generated by the pattern of channel opening shown in Fig. 9 *a*. The calculations were done twice (*a*) with the channel lifetime shortening as a function of the end-plate potential (Eq. 6), and (*b*) with channel lifetime unaffected by membrane potential. The voltage sensitivity of channel lifetime shortens the epc and the epp.

Fig. 10 shows the peak amplitude of calculated epps as a function of the number of channels opened in the end plate. Also shown are the corrections of epp amplitudes by Martin's method (1955). The correction of the realistic model, in which the channel lifetimes are shortened by depolarization, is excellent; the epp amplitude is directly proportional to the number of opened channels. When the voltage sensitivity of the channel lifetimes is eliminated, the method over-corrects by almost 10%.

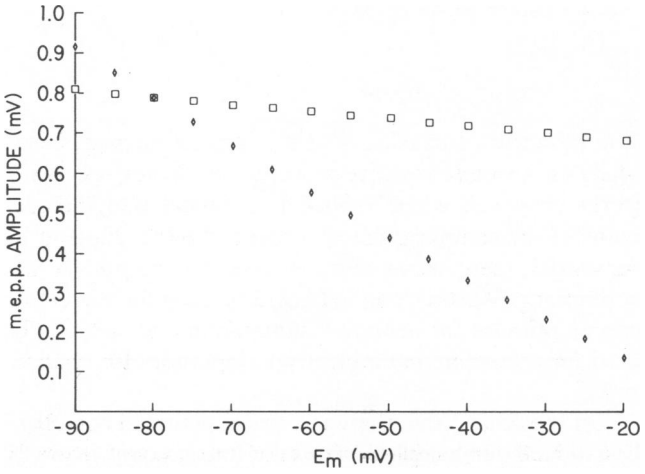

FIGURE 8 ◇, peak amplitudes of modeled miniature end-plate potentials at a series of different membrane potentials. □, amplitudes corrected by the method of Katz and Thesleff (1957) for a potential of −80 mV; *m.e.p.p.*, miniature end-plate potential.

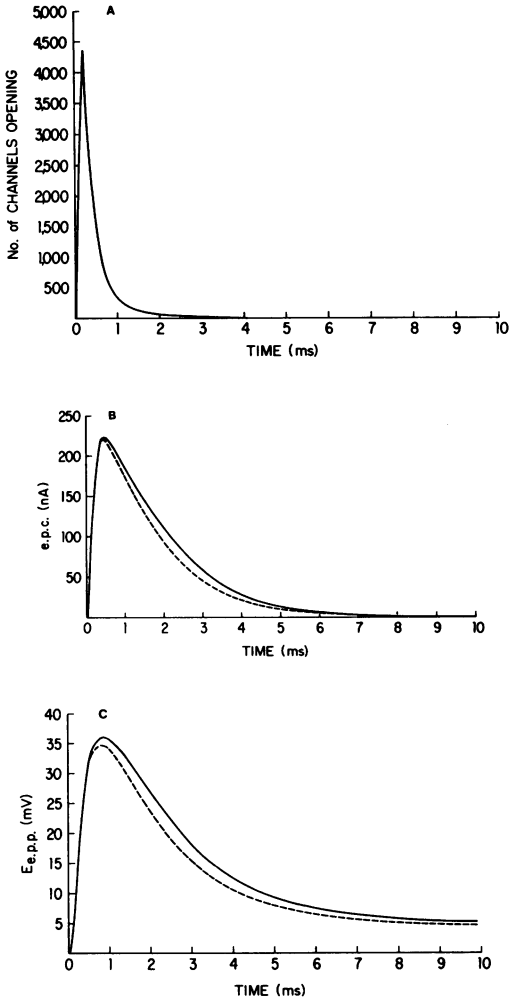

FIGURE 9 (*A*) The pattern of channel opening for the generation of an end-plate current. The method of calculation is described in the text. (*B*) The pattern of channel opening shown in Fig. 9 was used to calculate an epc. The dotted line shows the epc when the mean channel lifetime is a function of the membrane potential. The solid line is the epc when the mean channel lifetime is always that found at $E_m = -80$ mV. (*C*) The same calculations, but for an epp.

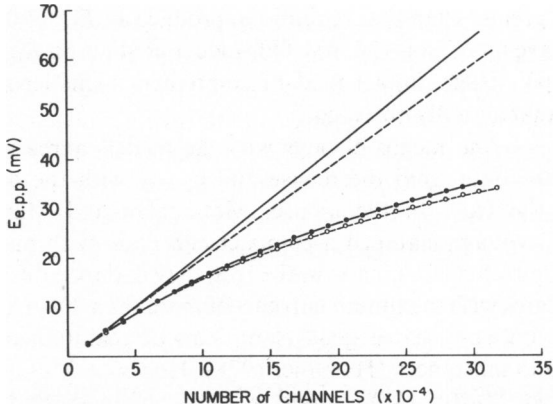

FIGURE 10 The relationship between the number of channels opening and the peak amplitude of the calculated epp. The dashed line with the open circles shows the calculations for channels that show the normal voltage dependency for their mean lifetimes. The correction by Martin's method (- - -) falls close to a linear relation between the peak amplitude and the number of channels. The solid line with filled circles shows the calculation with the mean channel lifetimes always that found at $E_m = -80$ mV. The solid line shows that Martin's method over-corrects when the channel lifetimes have a fixed duration.

CONCLUSIONS

The principal conclusion is that Martin's method, based solely on a simple resistive model of the motor end plate, works very well when applied to a model that includes many of the complications of a real end plate. Judging by the model, there seems to be no need for more elaborate corrections. Martin's method could be used for correcting epp amplitudes for nonlinear summation and can also be used for correcting miniature epp amplitudes for changes in E_m.

On the other hand, there is a major potential complication, which our model did not take into account, namely, the temporal dispersion of quantal releases following stimulation of the nerve. Part of the dispersion is due to the conduction times down the motor nerve terminals and to the time course of the secretion process (Katz and Miledi, 1965, 1967). This complication will be considered in a subsequent paper (Van der Kloot and Cohen, manuscript in preparation). Our model also did not take into account the evidence that the end-plate region has a higher input resistance than the rest of the muscle fiber (Miledi, 1960), and we have assumed the same properties for the T-system at the end plate as in the rest of the muscle.

The lifetime of the acetylcholine-gated channels at the end-plate membrane is shortened by depolarization. This behavior might be advantageous, since depolarization would favor the release of ACh from the receptor, and reduce the short-circuiting of the muscle membrane by the end plate (Lester et al., 1978). These factors may favor the evolution of channel voltage sensitivity, but the effect on currents or conductances is relatively small. In the example shown in Fig. 10, which is for a fairly large epp, the voltage is reduced by 12% by the voltage dependency of the channel lifetime.

Recently, McLachlan and Martin (1981) published the results of measurements at the same end plates of both epps and epcs. At the mouse end plate, a current six times greater than that required to give a 4.5 mV E_{epp} gives an E_{epp} of ~18.4 mV. Our model predicts an E_{epp} of ~18 mV. Almost the same value is predicted by an analytical cable model to a 1.5-ms depolarizing pulse (McLachlan and Martin, 1981; Ginsborg et al., 1981). For the mouse there is an excellent agreement between theory and experiment, and Martin's correction is quite effective.

McLachlan and Martin (1981) performed similar experiments on frog end plates. They found a linear relation between current and potential for E_{epp} up to ~10 mV. For higher amplitude E_{epp}, the potential was not directly proportional to the current, and Martin's method consistently over-corrected the amplitudes. A current 100

times greater than that required to produce an E_{epp} of 0.45 mV gave an E_{epp} of ~36 mV. Our model predicts an E_{epp} of ~30 mV. Their simpler model also predicts a smaller E_{epp} than that actually observed.

It is by no means obvious why the models agree well with the data from the mouse and poorly with the data from the frog. In the mouse, McLachlan and Martin (1981) voltage clamped a compact end plate with maximum currents of ~60 nA; in the frog they clamped diffuse end plates with maximum currents of more than 300 nA. It seems unlikely that a good clamp can be maintained in these circumstances (Hartline, 1978). However, McLachlan and Martin (1981) used a third voltage-recording electrode to check the effectiveness of their clamp at points along the fiber near the end plate and saw no indication of appreciable deviations from the clamped potential; and a faulty clamp would be expected to underestimate the current. Therefore, there is no evidence that the discrepancy between theory and experiment is due to technical difficulties.

McLachlan and Martin (1981) suggest that the problem with the frog comes from the diffuse end plate, which they could not model by their method. Our modeling shows that the diffuse end plate decreases the E_{epp} produced by a given current, so this is unlikely to be the explanation.

McLachlan and Martin (1981) also considered the effect of the voltage sensitivity of the channel lifetimes on the discrepancy between model and experiment. In the experiment, the fiber is voltage clamped, so the channel lifetimes are constant. In an unclamped preparation, the depolarization of the end plate shortens channel lifetimes so there is a reduction in the maximum current flowing, even though the same number of channels are opening. Therefore, the voltage sensitivity of the channel lifetimes should increase the discrepancy between model and experiment. Our calculations permit an evaluation of this additional discrepancy. In the example shown in Fig. 10, voltage dependence reduces the peak current by only 2%. But if the channel lifetimes are longer, both the peak current and the peak E_{epp} are decreased noticably.

We conclude that from the standpoint of a model of an end-plate on a muscle fiber, even one including all of the known complication, Martin's correction does very well in compensating for the effects of nonlinear summation. What remains unresolved is the relatively small discrepancy between theory and observation at the frog neuromuscular junction.

Supported by grant 10320 from the National Institute of Neurological and Communicative Disorders and Stroke and by the Muscular Dystrophy Association.

Received for publication 3 March 1983 and in final form 7 December 1983.

REFERENCES

Adams, W. B. 1976. Upper and lower bounds on the non-linearity of summation of end-plate potentials. *J. Theor. Biol.* 63:217–224.

Adrian, R. H., and W. Almers. 1973. Measurement of membrane capacity in skeletal muscle. *Nat. New Biol.* 242:62–64.

Adrian, R. H., and L. D. Peachey. 1973. The reconstruction of the action potential of the frog sartorius muscle. *J. Physiol.* (*Lond.*). 235:103–131.

Anderson, C. R., and C. F. Stevens. 1973. Voltage clamp analysis of acetylcholine produced end-plate current fluctuations at frog neuromuscular junction. *J. Physiol.* (*Lond.*). 235:655–691.

Bennett, M. R., T. Florin, and A. G. Pettigrew. 1976. The effect of calcium ions on the binomial statistical parameters that control acetylcholine release at preganglionic nerve terminals. *J. Physiol.* (*Lond.*). 257:597–620.

Carnahan, B., H. A. Luther, and J. O. Wilkes. 1969. Applied Numerical Methods. John Wiley and Sons, Inc., New York. 604.

Cohen, I. S., W. Van der Kloot, and D. Attwell. 1981. The timing of channel opening during miniature end-plate currents. *Brain Res.* 223:185–189.

Falk, G., and P. Fatt. 1964. Linear electrical properties of striated muscle fibers observed with intracellular electrodes. *Proc. R. Soc. Lond. Ser. B.* 159:69–123.

Fatt, P., and B. Katz. 1951. An analysis of the end-plate potential recorded with an intracellular electrode. *J. Physiol.* (*Lond.*). 115:320–370.

Gage, P. W., and R. S. Eisenberg. 1969. Capactitance of the surface and transverse tubular membrane of frog sartorius muscle fibers. *J. Gen. Physiol.* 53:265–278.

Ginsborg, B. L., E. M. McLachlan, A. R. Martin, and J. W. Searl. 1982. The computation of simulated endplate potentials. *Proc. R. Soc. Lond. Ser. B.* 213:233–242.

Hartline, F. F. 1978. Cable filtering and waveform variability of miniature end-plate currents at the frog neuromuscular junction. Ph.D. thesis, University of Washington, Seattle, Washington.

Katz, B., and R. Miledi. 1965. The effect of temperature on synaptic delay at the neuromuscular junction. *J. Physiol.* (*Lond.*). 181:656–670.

Katz, B., and R. Miledi. 1967. A study of synaptic transmission in the absence of nerve impulses. *J. Physiol.* (*Lond.*). 192:407–436.

Katz, B., and S. Thesleff. 1957. On the factors which determine the amplitude of the "miniature end-plate potential." *J. Physiol.* (*Lond.*). 138:267–278.

Lester, H. A., D. D. Koblin, and R. E. Sheridan. 1978. Role of voltage-sensitive receptors in nicotinic transmission. *Biophys. J.* 21:181–194.

Lewis, C. A. 1979. Ion-concentration dependence of the reversal potential and the single channel conductance of ion channels at the frog neuromuscular junction. *J. Physiol.* (*Lond.*). 286:417–455.

McLachlan, E. M., and A. R. Martin. 1981. Non-linear summation of end-plate potentials in the frog and mouse. *J. Physiol.* (*Lond.*). 311:307–324.

Magleby, K. L., and C. F. Stevens. 1972. A quantitative description of end-plate currents. *J. Physiol.* (*Lond.*). 223:173–197.

Martin, A. R. 1955. A further study of the statistical composition of the end-plate potential. *J. Physiol.* (*Lond.*). 130:114–122.

Martin, A. R. 1966. The effect of membrane capacitance on non-linear summation of synaptic potentials. *J. Theor. Biol.* 59:179–187.

McCracken, D. D., and W. S. Dorn. 1964. Numerical Methods and Fortran Programming. John Wiley and Sons, Inc., New York. 457.

Miledi, R. 1960. The acetylcholine sensitivity of frog muscle fibers after complete or partial denervation. *J. Physiol.* (*Lond.*). 151:1–23.

Moore, J. W., F. Ramon, and R. W. Joyner. 1975. Axon voltage-clamp simulations. I. Methods and tests. *Biophys. J.* 15:11–24.

Neher, E., and B. Sakmann. 1976. Noise analysis of drug induced voltage clamp currents in denervated frog muscle fibers. *J. Physiol.* (*Lond.*). 258:705–729.

Stevens, C. F. 1976. A comment on Martin's relation. *Biophys. J.* 16:891–895.

Takeuchi, A., and N. Takeuchi. 1960. On the permeability of the end-plate membrane during the action of transmitter. *J. Physiol.* (*Lond.*). 154:52–67.

Williams, J. D., and J. M. Brown. 1974. Effects of quantal unit latency on statistics of Poisson and binomial neuro-transmitter release mechanisms. *J. Theor. Biol.* 43:151–165.